The International Journal of Advanced Manufacturing Technology (2018) 97:267–278
https://doi.org/10.1007/s00170-018-1917-x

ORIGINAL ARTICLE

Experimental investigation of machinability in laser-assisted machining of fused silica

Huawei Song[1] · Jinqi Dan[1] · Xiao Chen[1] · Junfeng Xiao[1] · Jianfeng Xu[1]

Received: 27 October 2017 / Accepted: 15 March 2018 / Published online: 29 March 2018

Abstract
Fused silica is difficult to machine through conventional machining at room temperature, mainly due to high brittleness, low fracture toughness, high strength, and poor plastic deformation. In this study, we demonstrated experimentally that we are able to machine fused silica with improved efficiency and precision with laser-assisted machining (LAM) by heating workpiece locally in front of the cutting tool utilized a pulse CO_2 laser beam. Then, the machinability of fused silica was evaluated. The surface roughness tests with a Taguchi orthogonal array indicated that the pulse duty ratio was the main factor for a minimum Ra value achievement. The experimental results demonstrated a considerable improvement in the machinability of fused silica through the improved surface quality, high material removal rate, low rate of tool wear, as well as the cutting force reduction. The material removal mechanism was a hybrid of quasi plastic deformation and brittle fracture during the LAM of fused silica, which was inferred from the machined surface quality and chip morphology changes compared to the conventional machining.

Keywords Laser-assisted machining · Fused silica · Machinability · Surface quality · Cutting force

1 Introduction

Fused silica is an amorphous solid, composed of silicon dioxide, which constitutes an irregular link between silicon and oxygen atoms through the chemical bond formed non-crystalline structure that differs from the periodic network of crystal quartz. The non-crystalline structure form contributes in unique physical and chemical, mechanical and optical properties. In particular, the fused silica has an excellent spectral characteristic, which displays a strong permeability of the near-infrared to the ultraviolet light. Also, this material has a good corrosion resistance, reacting with no other acid substances than hydrofluoric acid. It was worth being mentioned that the corresponding chemical stability remains unmatched by any other engineering material at high temperatures [1]. With excellent physical and chemical properties, fused silica has a multitude of scientific and industrial applications in optical devices, precision instruments, high-power lasers, aerospace, and these application areas are constantly expanding [2]. Fused silica is difficult to machine with traditional cutting at room temperature, because it is a typical hard-brittle material resulting in machining difficult, due to high brittleness, low fracture toughness, and high strength [3].

Laser-assisted machining (LAM) is based on a laser as a heat source, where the beam is focused on the unmachined section of the workpiece [4]; the heated material is consequently removed in chips by the tool. This means that the previously heated material is sheared (Fig. 1). Most LAM applications are focused on machinability studies. It has been widely used in the processing of many different materials [5]. Generally, with the application of laser preheating, both the cutting force and tool wear are reduced and the material removal rate can be increased, compared to the conventional machining of the metal. Moreover, no coolant and special cutting tool necessity exists, which could cut down the costs by 50% [6] and produce significantly less pollution during LAM [7].

Anderson [8] reported of cutting experiments for the P550 stainless steel with LAM. The results demonstrated that the cutting energy was reduced by 25% as the temperature increased in the cutting zone and the tool life doubled, due to the material strength reduction. Compared to the traditional

✉ Jianfeng Xu
jfxu@hust.edu.cn

[1] State Key Laboratory of Digital Manufacturing Equipment & Technology, School of Mechanical Science and Engineering, Huazhong University of Science and Technology, 1037 Luoyu Road, Wuhan 430074, China

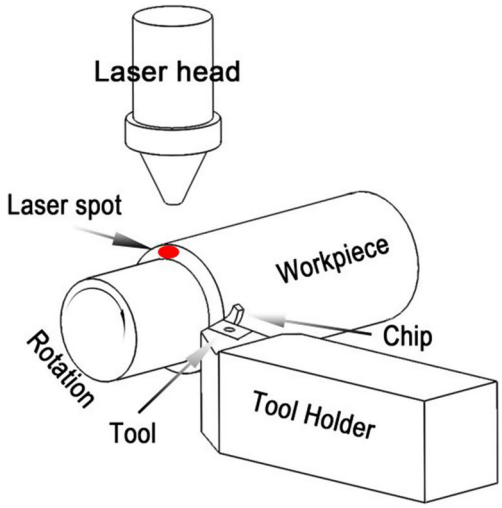

Fig. 1 Schematic of laser-assisted machining

cutting method, the subsurface structure and the hardness of the workpiece were nearly similar, where the processing duration was reduced by 20 to 50%. Masood S.H. [9] reported that the main cutting and feed forces were reduced by 24 and 22%, respectively, in the cutting experiments of white cast iron with LAM, whereas the microhardness of the workpiece surface was improved as the laser power increased. Sun [10] utilized LAM to investigate the cutting characteristics of pure titanium, which demonstrated that the cutting force was reduced by 20 to 50%. Under the comprehensive effect of lower dynamic cutting force and low hardness in the cutting zone, the surface quality was improved. As the cutting speed increased, the serrated chips transformed into continuous chips. In comparison with the results from the traditional cutting method, Rahman Rashid [11, 12] reported that the cutting force was reduced by 15% in the experiments of Ti-6Cr-5Mo-5V-4Al with LAM. Attia [13] investigated the cutting speed and feed rate effects on the quality during the machining of Inconel 718 with LAM. The cutting force decreased as the cutting speed increased and increased as the feed rate increased. The results demonstrated that the subsurface defects reached the lowest level and the material removal rate was improved by 800%, when the temperature ranged from 650 to 700 °C. Venkatesa [14–16] utilized the YAG laser in the Inconel 718 machining to investigate the irradiation angle effect on the surface temperature. The results indicated that the irradiation angle and the laser power were the most important factors that affected both the cutting force and the cutting temperature. The tool life was improved by 133% with LAM than the traditional machining method, where the cutting depth was set to 0.5 mm. Besides, the microhardness of the processed surface did not change and no subsurface defect was observed.

LAM technology improves the machinability performance of composites with high intense beam laser, to improve the thermal field of the composite matrices. Previous studies demonstrated that the LAM technology could reduce the cutting force, improving the tool life during complex materials processing. As an example, Wang [17] conducted the LAM of alumina reinforced composites. It was observed that the reinforced particles were pushed into the processed surface, due to the metal matrix softening, resulting in higher compressive residual stress during the laser assisted machining. Compared to the conventional machining, the cutting force was reduced by 30 to 50% and the tool life was increased by 20 to 30%. Danekar [18] observed that the processed subsurface damage increased in the LAM of long fiber composite materials. In contrast, the surface roughness was reduced by 65% and the damage decreased along with special cutting energy and tool wear. The parameter effects on the cutting force, the special cutting energy, the subsurface damage, and the tool wear were studied in the LAM of the A359/SiC metal matrix composite [19]. The results demonstrated that the surface roughness was reduced by 37%, the special cutting energy decreased by 12% and the tool life increased by 1.7 to 2.35 times. The polycrystalline diamond (PCD) tool was utilized for the laser assisted machining of ceramic particle reinforced titanium matrix by Beijian [20]. The tool life increased by 180% compared to the traditional turning. Consequently the cutting tool life mechanism through the chip morphology and microstructure observations was analyzed. The wear mechanism of cutting was conducted with cubic boron nitride (CBN) and carbide tool in the composite laser-assisted machining by Damian [21]. The results demonstrated that the failure mode of cutting was mainly wear in the flank, which decreased gradually as the temperature increased in the shear zone. The formation mechanism of the surface layer in the LAM of A359/20SiCp composite was researched through both theoretical study and experimentation. The surface roughness decreased by 32% and the tool wear decreased by 27% compared to conventional machining [22]. It was discovered that the abrasion resistance of the material was improved through the cutting tool and laser spot adjustments. Kong [23] investigated the laser-assisted machining of metal matrix composites utilizing a 100W semiconductor laser. The L_9 (3^4) orthogonal matrix was used to test the relationship between the surface roughness and the parameters including depth of cut, feed rate and rotation speed. The combination of optimal parameters was obtained through analysis of variance (ANOVA), when the surface roughness reached the corresponding minimum.

The LAM constitutes the ceramic cutting of feasible and machining efficiency to increase and produce good surface quality without cracks. This indicates that the machinability of the ceramics would be improved, in comparison with conventional machining.

Rozzi [24], Lei [25], Patrick [26], and Korn [27] studied the Si_3N_4, ZrO_2 and mullite ceramic with numerical

simulations and extensive experimental investigation. The physical and mathematical model of the three-dimensional transient temperature field was built and the workpiece surface temperature change during cutting was analyzed and predicted, according to the original test curve. During machining experimentation, the machining parameters effects were analyzed, which indicated that the cutting force and the tool wear decreased as the machining temperature increased. It could also be observed that residual compressive stress on the machined surface existed, which contributed in the formation and expansion inhibition of microcracks, improving the fatigue life and tensile strength of the material. In contrast, the stress was slightly lower than the residual compressive stress during grinding. Chang [28] conducted an experimentation of an Al_2O_3 ceramic turning with laser-assisted machining. Based on the experimental results, the orthogonal method was utilized to optimize the machining parameters to achieve the minimum roughness. Also, an empirical model of the relationship among the cutting speed, the depth of cut, the feed rate, the laser frequency and the surface quality was established. It was discovered that the cutting speed was the main parameter affecting the surface quality, followed by the feed rate and the depth of cut, whereas the laser frequency had the lowest effect. Kuo [29] found that LAM could highly improve the material removal rate and reduce the machined surface roughness, when LAM was utilized in the Al_2O_3 ceramic machining. Jong [30] utilized a high-energy semiconductor to assist the Si_3N_4 ceramic machining. It was indicated that the cutting force increased and the tool life decreased as the feed rate and depth of cut both increased, whereas the maximum depth of cut could reach up to 3 mm. The machining Si_3N_4 ceramic mechanism was clarified in the LAM. Roostaei [31] utilized the solid-state laser YAG to assist the fused silica ceramic turning, and consequently the three-dimensional transient heat transfer model was built through the finite element method and the laser effect on the material removal mechanism was analyzed, which was verified in the experiment.

In summary, the successful application of LAM in the machining of ceramic materials provided a valuable reference for the LAM technology application in the fused silica processing, due to both hardness-brittleness existence as well as difficulty in machining, due to the non-metallic structure. In contrast, the LAM of fused silica has never been conducted before. In the present investigation, the turning processing technology of fused silica was attempted to be explored with the pulse CO_2 laser assistance application. The object of this study was the machinability characteristics research of fused silica during the LAM, including surface quality, material removal rate, chip morphology, tool wear, and cutting forces. Consequently, the material removal mechanism was analyzed.

2 LAM experimental procedure

2.1 Experimental setup and processing

The experimental system for the LAM of fused silica included a CO_2 technological laser (SR10i, ROFIN), which delivered a power range of 5 to 125 w. The maximum pulse duty ratio of 60% and the wavelength of 10.6 μm were utilized for the experiments. The ranges of the parameters were 0–130 kHz for the pulse frequency, 2–400 μS for the pulse width and 5–100 mJ for the pulse energy. The laser was connected to a machining system with three translational and one rotational motions, which was designed specifically on the basis of the universal NC machine tool. The laser head was mounted on a mechanical unit that changed the position of the beam and the corresponding spot size was ahead of the cutting tool. The laser beam was delivered by an optical system, which was consisted of the reflecting mirror, the laser beam expanders and the focusing lens. The laser beam of 3 mm in spot size was utilized, through the positive defocusing distance adjustment of the focusing lens at 63.5 mm, where the workpiece surface was irradiated 180 degrees in the circumferential, ahead of the cutting tool. Compressed air under pressure of 0–0.6 MPa was utilized to protect the laser lens from excess heat and chips. The laser-assisted machining is illustrated in Fig. 2.

The turning tests were carried out with cylindrical fused silica workpieces, approximately 10 mm in diameter and 35 mm in length during each experiment. Approximately 25 mm of the material length were machined with a DCMT11T304 poly crystalline diamond (PCD), with a tool nose radius of 0.4 mm that was mounted on the standard tool holder model of SDJCR2020k11. To minimize the workpiece runout, a three-jaw chuck held the workpiece. During the machining tests, the cutting force response on the cutting tool was measured with a three component Kistler dynamometer (type

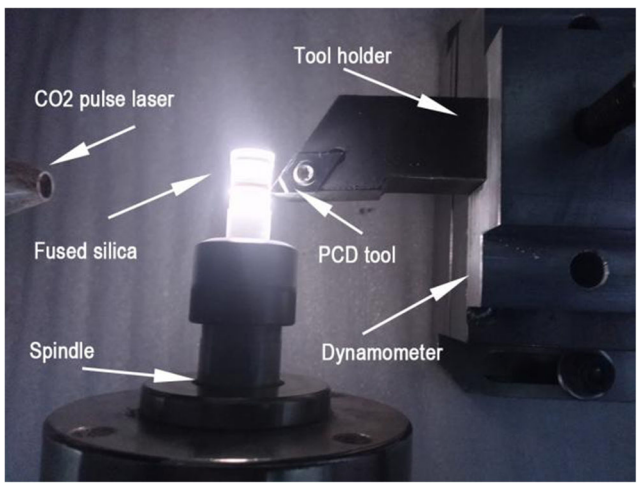

Fig. 2 Experimental system for LAM of fused silica

Table 1 Experimental operating conditions for surface roughness

Process parameter	Unit	Level 1	Level 2	Level 3	Level 4
Rotation speed (A)	rpm	480	540	600	660
Feed rate (B)	mm/s	0.05	0.1	0.15	0.2
Depth of cut (C)	μm	2	4	6	8
Pulse duty ratio (D)	percentage	35%	40%	45%	50%

9257A). For each experiment, the tool wear was measured with a microscope (type scopeimage-9.0). The surface roughness values of the machined surfaces were measured by the arithmetic average deviation (Ra) at the end of the cut. A transverse length of 0.8 mm and a cutoff length of 4.8 mm were utilized for each measurement (Mitutoyo, SJ-410), along the direction in parallel to the axis of the cylindrical workpiece surface and the average value of the Ra was calculated from a three time average. The chips were collected and the morphology of the machined surface subsequently to being coated with gold was examined with a scanning electron microscope (model: Helios, NanoLab, G3, CX).

2.2 Methodology

The Taguchi method is a powerful statistical technique for product quality improvement. This methodology aims at the optimal process parameter setting identification so as to obtain the variation in response, due to the noise factors being eliminated [32]. Two major tools that were utilized in the Taguchi optimization methodology were the orthogonal arrays (OAS) and the signal-to-noise (S/N) ratio. The OAS was used to examine the influence of parameters on quality characteristics through a minimum number of experiments. It accommodated multiple design factors at the same time and each factor can be evaluated independently from other factors [33]. The S/N ratio was a quantitative analysis tool, in which the signal represents the desirable value and noise represents the undesirable value. It was a measure of the quality characteristic deviation from the desired value. There are three different quality characteristics models in S/N ratio: smaller-the-better, larger-the-better, and nominal-the-best [34]. In this study, the output response values of surface roughness need to be minimum, so the

Table 2 L_{16} (4^4) orthography array and calculated observed values

Trial no.	Process parameters and levels				Experimental results					Signal-to-noise ratio	
	A Rotation speed (rpm)	B Feed rate (mm/s)	C Depth of cut (μm)	D Pulse duty ratio (%)	MRR ($\times 10^{-3}$ mm^3/s)	Tool wear VBc (μm)		Surface roughness Ra (μm)		Surface roughness S/N ratio (dB)	
						CM	LAM	CM	LAM	CM	LAM
1	1 (480)	1 (0.05)	1 (2)	1 (35%)	3.01	124.99	118.81	2.49	1.58	− 7.92	− 3.97
2	1	2 (0.10)	2 (4)	2 (40%)	12.07	168.19	126.57	3.29	1.50	− 10.34	− 3.52
3	1	3 (0.15)	3 (6)	3 (45%)	27.13	199.07	134.24	2.83	1.00	− 9.04	0.00
4	1	4 (0.20)	4 (8)	4 (50%)	48.23	225.33	140.42	3.08	1.21	− 9.77	− 1.66
5	2 (540)	1	2	3	6.03	243.88	148.14	1.88	1.03	− 5.48	− 0.26
6	2	2	1	4	6.03	263.85	158.94	2.60	0.92	− 8.30	0.72
7	2	3	4	1	36.17	273.22	166.65	2.87	1.04	− 9.16	− 0.34
8	2	4	3	2	36.17	283.96	174.54	3.31	1.53	− 10.40	− 3.69
9	3 (600)	1	3	4	9.042	302.43	180.70	2.17	1.07	− 6.73	− 0.59
10	3	2	4	3	24.11	316.33	188.31	2.77	1.30	− 8.85	− 2.28
11	3	3	1	2	9.04	327.12	197.60	3.82	1.43	− 11.64	− 3.11
12	3	4	2	1	24.12	336.38	205.24	3.69	1.45	− 11.34	− 3.23
13	4 (660)	1	4	2	12.06	347.21	214.65	2.19	1.18	− 6.81	− 1.44
14	4	2	3	1	18.09	358.06	220.80	2.20	1.84	− 6.85	− 5.30
15	4	3	2	4	18.09	364.21	227.02	3.72	1.27	− 11.41	− 2.08
16	4	4	1	3	12.06	370.44	230.08	3.93	1.67	− 11.89	− 4.45

smaller-the-better type of the S/N ratio has been used and defined as follows:

$$S/N = -10\log_{10}\left(\frac{1}{n}\sum_{1}^{n} y_i^2\right) \quad (1)$$

where S/N represents the response values (dB) and y_i is the observed value of the machining characteristic under a trial condition repeated for n times.

2.3 Experimental design

Many factors affect the characteristics of laser-assisted machining, including the process and the laser system. In the traditional turning process, rotation speed, feed rate, and depth of cut were the main process parameters which affected performance characteristics. The laser power could affect the distribution of temperature field in the workpiece surface which had significant influence on machining, and it was determined by the pulse duty ratio and laser frequency. Hence, rotation speed, feed rate, depth of cut, and pulsed duty ratio were selected as four main factors.

In the first step, minimum surface roughness was set as the objective function of experiment. L_{16} (4^4) standard orthogonal array matrix was constructed as the experimental design in accordance with TM; each parameter had four levels, as shown in Table 1. The other parameters were set to a fixed value as beam spot diameter of 3 mm, focal length of 63.5 mm, and laser irradiation angle of 180°. In the second step, the minimum cutting force is the objection function. The cutting force was obtained by using similar experiment process in the first step. Then, analysis of variance (ANOVA) and S/N ratio were used to analyze experimental data.

3 Results and discussion

3.1 Analysis of variance

According to the Taguchi method theory, the analysis of variance (ANOVA) was performed to study the effect of the machining parameters, which represented the relationship among the rotation speed, the feed rate, the depth of cut, and the pulse duty ratio as well as the observed values.

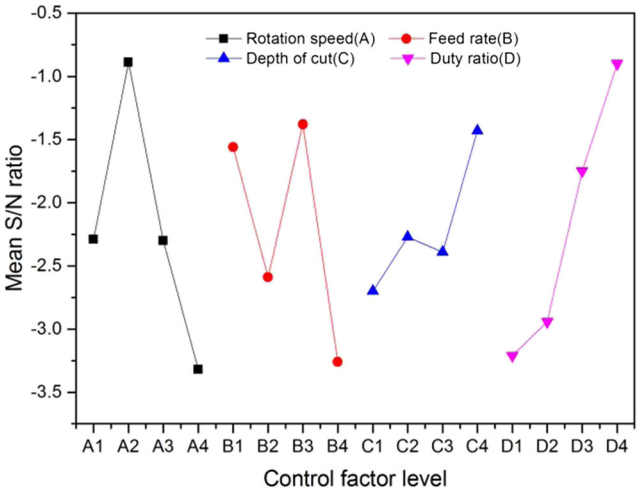

Fig. 3 Mean signal-to-noise for each factor

As presented in Table 3, the ANOVA for different factors enabled various relative quality effects to be determined on the basis of calculated S/N ratio values presented in Table 2, which included the degree of freedom, the sum of square, the sum of mean square and the contribution.

3.1.1 Contribution of each factor

Regarding percentage contribution, it could be observed that the contribution percentages were the rotation speed, the feed rate, the depth of cut and the pulse duty ratio at 28.89%, 24.44%, 12.22%, and 34.44%, respectively (Table 3). Consequently, it could be concluded that the pulse duty ratio had a dominant effect on the mean value of the surface roughness. This could be explained by the fact that the size and degree of softening in the cutting zone became apparent, where the hardness and strength of the material were reduced, due to the temperature of the material before the cutting tool point by the high energy laser beam. The contribution percentage for the depth of cut was the lowest at 12.22%, probably because the temperature decreased within the material towards the depth direction by pulse laser irradiation, leading the preheating to become deficient and the workpiece not to be sufficiently softened.

Table 3 Analysis of variation

Factor	D.O.F	Sum of square	Sum of mean square	Contribution
A	3	0.26	0.09	28.89%
B	3	0.22	0.07	24.44%
C	3	0.11	0.04	12.22%
D	3	0.31	0.11	34.44%
Total	15	0.90	0.36	100%

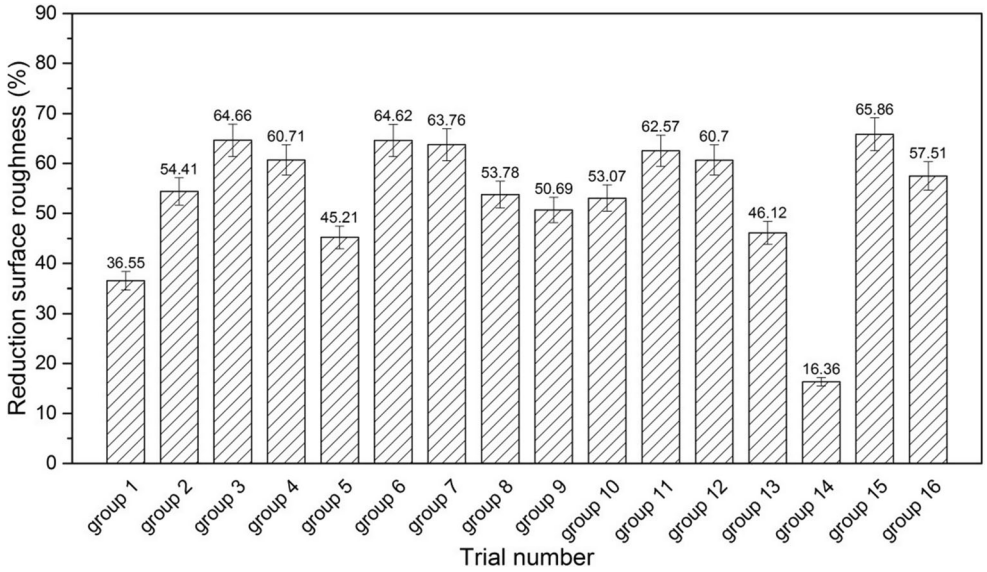

Fig. 4 Percentage reduction of surface roughness for cutting conditions trial 1–16

3.1.2 Optimum condition

The S/N ratio of the levels for each factor can be calculated individually, as presented in Table 2. Then, the mean S/N ratios of each factor were calculated by averaging at corresponding levels. Then, the main effect plots of these levels were also used for the evaluation (Fig. 3). The response value was changed when the given factor increased from the lower level to the higher level. According to the principle of the smaller-the-better, the corresponding level value of the high S/N ratio was selected as the optimal machining condition.

It can be seen in Fig. 3 that the surface roughness was minimal at the second level of rotation speed (A), third level of feed rate (B), fourth level of depth of cut (C), and fourth level of pulse duty cycle (D). Thus, the optimal parametric combination for minimum surface roughness was determined to be A2B3C4D4 with a rotation speed of 540 rpm, feed rate of 0.15 mm/s, depth of cut of 8 μm, and pulse duty ratio of 50%.

3.1.3 Surface roughness and material removal rate

Upon completion of the experimental matrix, the surface roughness and the material removal rate parameters were measured and calculated. The surface roughness was significantly in conventional machining and could be observed in Fig. 4, when it is compared to LAM under the same condition. The results demonstrated a maximum reduction in surface roughness of approximately 65.86%. In fact, the beam irradiation increased the local temperature, consequently the wear rate of tool decreased, resulting in an improved surface roughness, as further demonstrated. A minimum reduction of surface roughness is 16.36% (group14), that is because the duty ratio is 35% in the

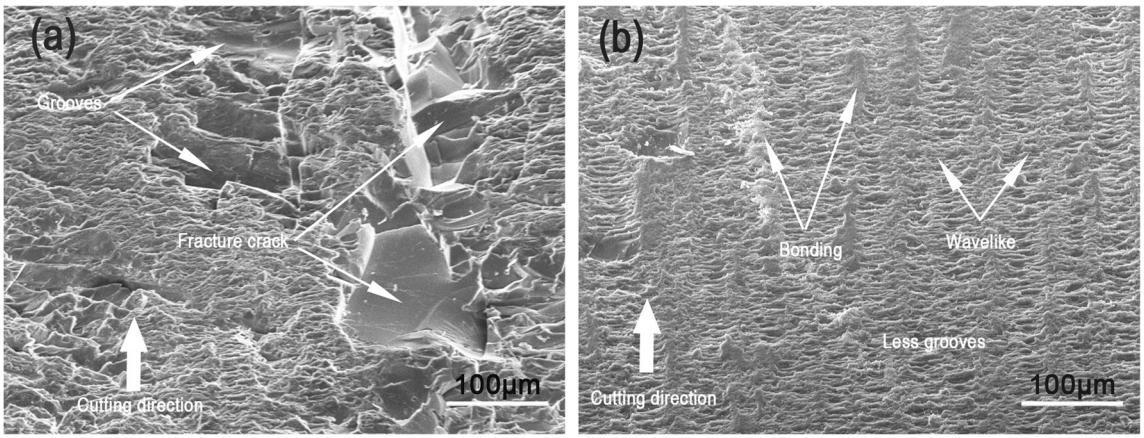

Fig. 5 SEM image of workpiece surface during **a** conventional machining and **b** LAM

combination parameters, which means the workpiece was not sufficiently softened.

In the case of the same material removal rate, the lower surface roughness could be obtained with LAM compared to conventional machining (Table 2). A low depth of cut and the feed rate process parameters are required in order to obtain a lower surface roughness during conventional machining. This meant that the same surface roughness was aimed to be obtained with laser assisted machining, where the depth of cut or the feed rate must be reduced in the conventional machining, leading to the material removal rate decrease. Therefore, the LAM technology could increase the removal rate of the material, improving the production efficiency and cost saving.

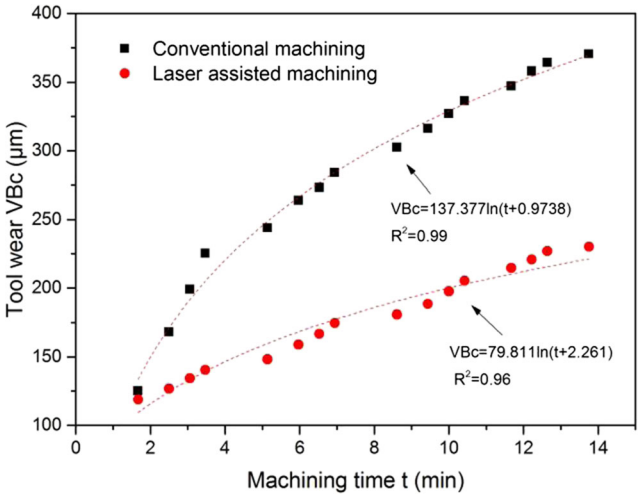

Fig. 7 Variation of average tool wear for PCD tool as function of machining time

3.2 Material removal mechanism

The best evidence of the materials removal mechanisms during LAM of fused silica were observed in the surface morphology of the cutting zone.

The conventional machining surface demonstrated a high number of high-sized grooves, whose size is approximately 150 μm, due to brittle fracture movement, oriented in the direction of the tool movement, as evidence of fracture deformation in the conventional machining of fused silica (Fig. 5a). In the LAM surface, a marked decreased in the number of fracture locations and bonding wavelike texture appeared which signified a workpiece deformation behavior change by the local temperature of the material in front of the cutting tool (Fig. 5b). These differences were indicative of quasi plastic deformation as the predominant mode of material removal near the last point of the tool contact region during the LAM of fused silica.

Brittle fracture was the main deformation mode in the conventional machining of fused silica, if the produced cracks in the cutting zone were created continuously, reducing the strength to the material significantly at the machining interface. High-sized pieces of material could consequently be removed by fracture before the yield stress was reached, which was consistent with the large-scale fracture segment chip (Fig. 6a).

The chips were collected and coated with gold for the SEM investigation, resembling the chips produced form conventional metal machining processes, with the high-sized semi continuous (size is approximately 20 μm) and some fragmentation chips (Fig. 6b). The low-sized fragmented chips (the maximum size of chip about 10 μm) were possibly associated with the occurrence of a certain amount of brittle fracture. In this case, the semi continuous chips were most likely produced from the breakup of high-sized chips by the micro brittle fracture, immediately following material removal. This occurred because as the material removal temperature increased, the fused silica material viscosity decreased during LAM, resulting in the chip formation through viscoplastic deformation under the advancement of the cutting tools, when the materials reached the cutting tool. As the chips gradually broke away from the high temperature zone, which were cooled by air resulting in a high

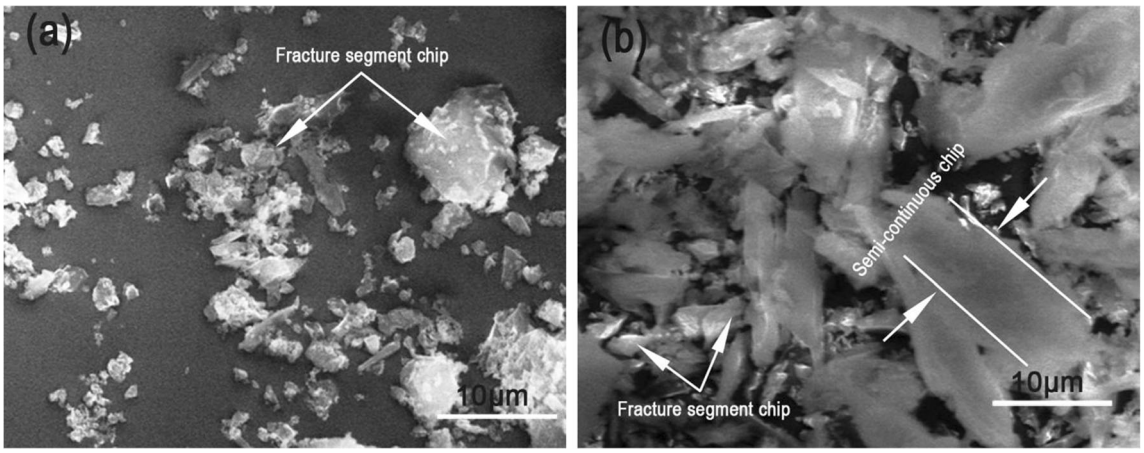

Fig. 6 SEM image of chip characteristics during **a** conventional machining and **b** LAM

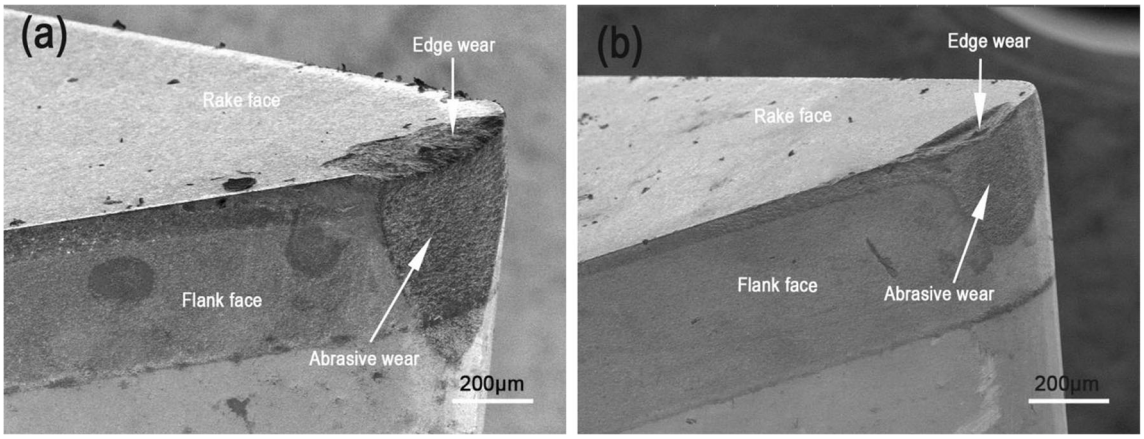

Fig. 8 SEM image of PCD tool following machining: **a** conventional machining and **b** LAM

temperature gradient, due to the sharp reduction of temperature outside the cutting zone, which caused a high amount of thermal stress and deformation of the morphology. Semi-continuous chips would be obtained due to breakage, when the degree of deformation exceeded the fracture strain of the material [27]. Consequently, both the machined surface and chip morphology suggested that the material removal mechanism was a hybrid of plastic deformation and brittle fracture. In contrast, unlike conventional ductile region machining, the bulk of the material was removed by the combination of fracture and plastic deformation ahead of the last point of the tool contact, resulting in a high material removal rate.

3.3 Tool wear

Figure 7 presents the LAM effect on the tool wear with the PCD tool. The fused silica had poor machinability during conventional machining. As a consequence of heating, the tool wear decreased in comparison with conventional machining, during the 14 min of machining (Fig. 8). The PCD tool utilized in LAM demonstrated a significantly longer tool life compared to the conventional machining of fused silica at the same cutting condition. These results could be easily explained by an increase in the workpiece temperature beyond the material yield temperature in the cutting zone with laser assistance, which facilitated the plastic deformation of fused silica.

The cutting tool edge utilized in the conventional machining and LAM is presented in Fig. 8, which indicates grooves on both the rake and flank faces due to abrasion. A close examination under the optical microscope displayed a slight edge wear on the rake face of the PCD tool at high temperature during the LAM (Fig. 8b). In contrast, edge wear widely occurred during the conventional machining within lower material temperature range (Fig. 8a). In addition, the tool wear on the flank face was quite noticeable and non-uniform along the cutting edge. The maximum occurrence near the middle

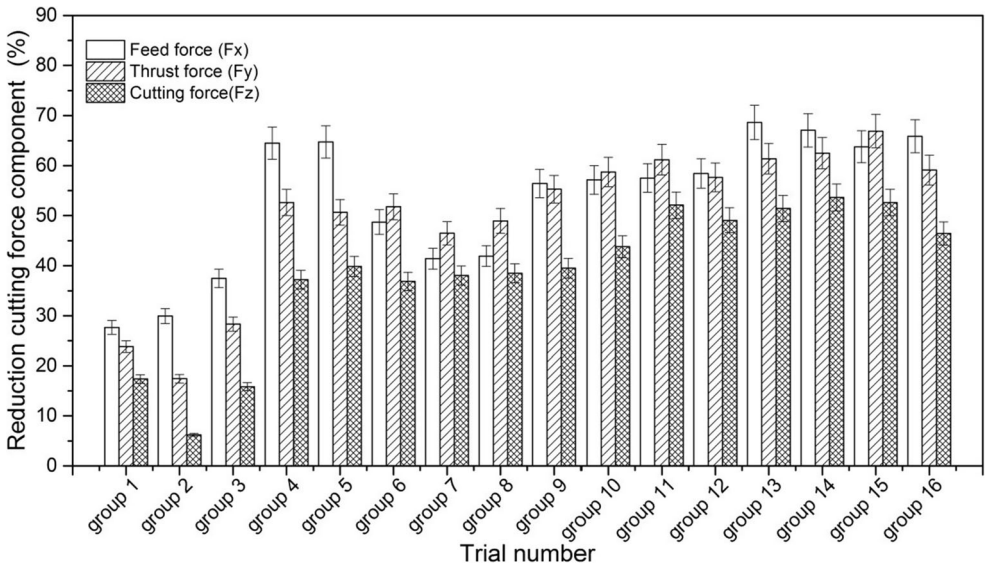

Fig. 9 Cutting force component reduction obtained by convention machining vs LAM

Table 4 L_{16} (4^4) orthography array for comparative results of LAM vs conventional machining

Trial no.	A Rotation speed (rpm)	B Feed rate (mm/s)	C Depth of cut (μm)	D Pulse duty ratio (%)	Comparative results CM vs LAM								
					Feed force (Fx N)			Thrust force (Fy N)			Cutting force (Fz N)		
					CM	LAM	Delta (%)	CM	LAM	Delta (%)	CM	LAM	Delta (%)
1	1 (420)	1 (0.20)	1 (20)	1 (35%)	1.36	0.99	27.21	15.19	11.57	23.83	12.30	10.16	17.40
2	1	2 (0.25)	2 (22)	2 (40%)	1.47	1.03	29.93	17.28	14.27	17.42	13.93	13.07	6.17
3	1	3 (0.30)	3 (24)	3 (45%)	1.82	1.14	37.36	24.60	17.63	28.33	18.41	15.49	15.86
4	1	4 (0.35)	4 (26)	4 (50%)	2.55	0.91	64.31	33.46	15.86	52.60	24.49	15.38	37.20
5	2 (480)	1	2	3	2.65	0.93	64.91	26.87	13.26	50.65	20.07	12.07	39.86
6	2	2	1	4	1.75	0.90	48.57	23.49	11.33	51.77	17.58	11.10	36.86
7	2	3	4	1	2.30	1.35	41.30	27.95	14.95	46.51	20.36	12.61	38.06
8	2	4	3	2	2.50	1.45	42.00	33.44	17.06	48.98	23.79	14.63	38.50
9	3 (540)	1	3	4	2.87	1.25	56.45	29.87	13.36	55.27	20.81	12.59	39.50
10	3	2	4	3	2.62	1.12	57.25	33.20	13.71	58.70	22.76	12.79	43.80
11	3	3	1	2	2.32	0.98	57.76	31.33	12.17	61.16	22.04	10.56	52.09
12	3	4	2	1	2.51	1.04	58.57	31.09	13.17	57.64	21.70	11.05	49.08
13	4 (600)	1	4	2	2.98	0.93	68.79	27.75	10.72	61.37	19.30	9.38	51.40
14	4	2	3	1	2.59	0.85	67.18	28.52	10.70	62.48	19.52	9.06	53.59
15	4	3	2	4	2.60	0.94	63.85	29.44	9.75	66.88	20.28	9.61	52.61
16	4	4	1	3	2.55	0.87	65.88	30.44	12.45	17.99	20.78	11.13	9.65

portion of the edge, due to the brittle fracture of the PCD tool at a certain point during machining, resulted in deterioration of the tool geometry.

Flank wear measurements were also obtained from the cutting tools. The average tool wear VBc was 370.44 μm in conventional machining and 230.08 μm in the flank face during the LAM. It could be concluded that the LAM outperformed the conventional machining by approximately 38.79% in terms of flank wear.

Abrasion, adhesion, and diffusion were the primary tool wear mechanisms during the LAM of fused silicon. Furthermore, the flank wear was the dominant tool failure mode, which was attributed to the fused silica semi liquid adhesion of the PCD tool during LAM [21].

3.4 Cutting force

3.4.1 Cutting force component

The percentage reduction of the force component was calculated for each experiment (Fig. 9). From all experiments, it could be noted that a reduction in the cutting forces existed in

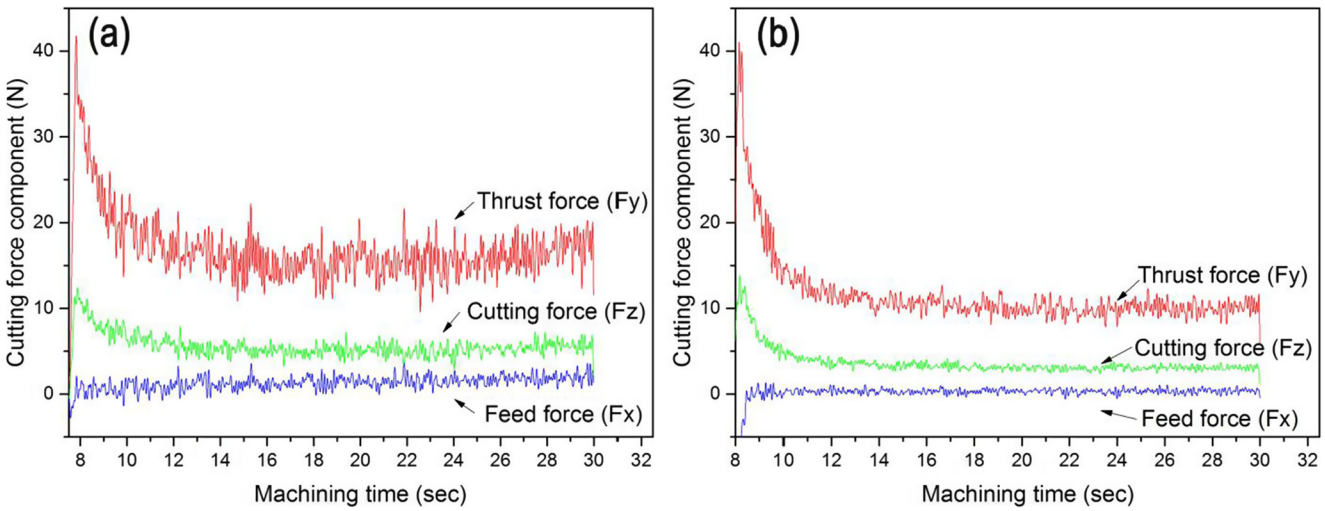

Fig. 10 Force fluctuations for LAM: **a** conventional machining and **b** LAM

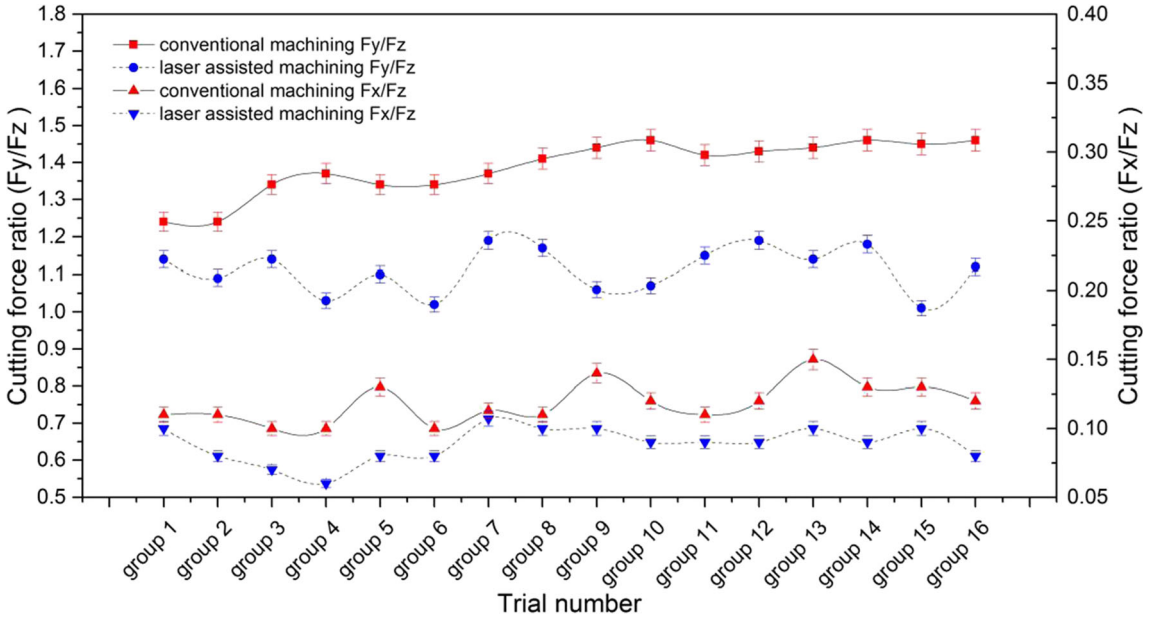

Fig. 11 Ratio of cutting force for fused silica by conventional machining vs LAM

LAM, when it was compared to conventional machining. Based on the obtained results, it could be observed that the percentage reduction of the forces in LAM were in the ranges of 27.66–68.64% for the feed force, 17.43–66.89% for the thrust force, and 6.2–53.61% for the cutting force, compared to the conventional machining from Table 4.

These could be explained by the fact that the cutting force was reduced through cutting by plastic deformation, as the workpiece surface was preheated and softened due to high temperature. On the other hand, physical phenomena, such as evaporation and vaporization by laser irradiation existed, that decreased the thickness of the cutting layer during the LAM, which subsequently reduced the cutting forces.

Simultaneously, the chattering decreased in the LAM of fused silica as the temperature increased (Fig. 10b). This occurred because the preheating of the workpiece surface with the laser beam prior to cutting tool contributed in the reduction of the cutting forces at the cutting edge, during machining. In addition, based on the aforementioned analysis, the improved tip geometry of the tool resulted in a lower chattering. As the chattering decreased, the surface roughness of the machined surface was also improved [30].

3.4.2 Specific ratio of cutting force

Figure 11 presents the specific ratio cutting force components during LAM compared to the conventional machining. It was observed that a specific ratio reduction of the cutting forces for all experiments existed. Specifically, the average value of Fy/Fz was 1.39 and 1.11 corresponding to the average value of Fx/Fz of 0.12 and 0.09 in conventional machining and LAM, respectively.

During the LAM of mullite ceramics [35], the transition points among brittle fracture, semi continuous and continuous chip formation were inferred from specific cutting force ratio. When Fy/Fz is less than 1, semi continuous chips forms, which is a consequence of plastic deformation in the LAM process due to the softening effect of high intense laser. As aforementioned, similar semi-continuous chips were obtained corresponding to the average value of Fx/Fz is 0.09, which meant that quasi plastic deformation occurred in the LAM of fused silica. According to the cutting theory, the Fy/Fz represented the friction coefficient. As the average values of Fy/Fz were reduced compared to the conventional machining, the friction decreased in the LAM.

4 Conclusions

This study was the first attempt to explore the machinability of fused silica with laser assisted machining, which includes surface quality, the chip morphology, the tool wear, and the cutting forces. The surface roughness tests with the taguchi orthogonal array indicated that the pulse duty ratio was the main factor for a minimum Ra value achievement, whereas the contribution percentages of the pulse duty ratio, the rotation speed, the feed rate, and the depth of cut were 34.44%, 28.89%, 24.44%, and 12.22%, respectively. In addition, the optimum machining condition must be properly correlated with the other machining parameters as pulse duty ratio of 50%, rotation speed 540 r/min, feed rate of 0.15 mm/s, and depth of cut of 8 μm.

A high number of grooves was produced in the machined surface, due to the brittle fracture movement in conventional

machining. During the LAM of fused silica, the bonding texture in the machined surface indicated a behavior change of workpiece deformation by the local temperature of the material in front of the cutting tool. The semi continuous chips were obtained, which constituted the material removal mechanism evidence as a hybrid of quasi plastic deformation and brittle fracture. The interaction mechanism of the laser and the material were combined with a cutting model, to provide a full analysis of the LAM, which was the next step in the present research.

At the same cutting condition, the average tool wear was 370.44 μm in conventional machining and 230.08 μm in the LAM, which illustrated that the tool life was improved by approximately 38.79%. Gradual flank wear was the dominant tool failure mode leading to the tip geometry of the tool to improve, which resulted in a lower chattering during LAM. As the chattering decreased, the surface roughness of the machined surface was reduced by approximately 65.86% at maximum. Furthermore, the cutting force reduction of 27.66–68.64% in the feed direction, 17.43–66.89% in the thrust direction, and 6.2–53.61% in the main cutting force on the cutting tool were observed from all the experiments.

It was clearly indicated that LAM was a potential economically viable processing technique for fused silica with improved surface quality, high material removal rate, low rate of tool wear, and reduction of cutting forces which could be possibly applied to other difficult to machine materials.

Acknowledgements The authors thank the Analytical and Testing Center of Huazhong University of Science and Technology. The authors also thankful to Ms. Yan Zhu for providing help for the measurement of surface roughness of the workpiece for research work.

Funding information This work was supported by the National Natural Science Foundation of China (grant no. 51375195) and China Postdoctoral Science Foundation (grant no. 2017 M612447).

References

1. Hawleyfedder RA, Stolz CJ, Menapace JA, Borden MR, Yu J, Runkel MJ, Feit MD (2004) NIF optical materials and fabrication technologies: an overview. Proc SPIE Int Soc Opt Eng 5341:102–105
2. French RH, Tran HV (2009) Immersion lithography: photomask and wafer-level materials. Annu Rev Mater Res 39(1):93–126
3. Zhou C, Zhang Q, He C, Li Y (2014) Function of liquid and tool wear in ultrasonic bound-abrasive polishing of fused silica with different polishing tools. Opt Int J Light Electron Opt 125:4064–4068
4. Ding H, Shin YC (2013) Improvement of machinability of Waspaloy via laser-assisted machining. Int J Adv Manuf Technol 64:475–486
5. Lei S, Pfefferkorn F (2007) A review on thermally assisted machining: ASME 2007 International Manufacturing Science and Engineering Conference, pp. 325–336
6. Anderson M, Patwa R, Shin YC (2006) Laser-assisted machining of Inconel 718 with an economic analysis. Int J Mach Tool Manu 46:1879–1891
7. Zhao F, Bernstein WZ, Naik G, Cheng GJ (2010) Environmental assessment of laser assisted manufacturing: case studies on laser shock peening and laser assisted turning. J Clean Prod 18:1311–1319
8. Anderson MC, Shin YC (2006) Laser-assisted machining of an austenitic stainless steel: P550. Proc Inst Mech Eng B J Eng Manuf 220:2055–2067
9. Masood SH, Armitage K, Brandt M (2011) An experimental study of laser-assisted machining of hard-to-wear white cast iron. Int J Mach Tools Manuf 51:450–456
10. Sun S, Harris J, Brt M (2010) Parametric investigation of laser-assisted machining of commercially pure titanium. Adv Eng Mater 10:565–572
11. Rahman Rashid RA, Bermingham MJ, Sun S, Wang G, Dargusch MS (2013) The response of the high strength Ti–10V–2Fe–3Al beta titanium alloy to laser assisted cutting. Precis Eng 37:461–472
12. Rahman Rashid RA, Sun S, Wang G, Dargusch MS (2012) An investigation of cutting forces and cutting temperatures during laser-assisted machining of the Ti–6Cr–5Mo–5V–4Al beta titanium alloy. Int J Mach Tools Manuf 63:58–69
13. Attia H, Tavakoli S, Vargas R, Thomson V (2010) Laser-assisted high-speed finish turning of superalloy Inconel 718 under dry conditions. CIRP Ann Manuf Technol 59:83–88
14. Venkatesan K, Ramanujam R, Kuppan P (2014) Analysis of cutting forces and temperature in laser assisted machining of Inconel 718 using taguchi method. Procedia Engineering 97:1637–1646
15. Venkatesan K, Ramanujam R (2015) Improvement of machinability using laser-aided hybrid machining for Inconel 718 alloy. Advanced Manufacturing Processes 31(14):1825–1835
16. Venkatesan K, Ramanujam R (2016) Statistical approach for optimization of influencing parameters in laser assisted machining (LAM) of Inconel alloy. Measurement 89:97–108
17. Wang Y, Yang LJ, Wang NJ (2002) An investigation of laser-assisted machining of Al2O3 particle reinforced aluminum matrix composite. J Mater Process Technol 129:268–272
18. Dandekar CR, Shin YC (2010) Laser-assisted machining of a fiber reinforced metal matrix composite. J Manuf Sci Eng 132:61004
19. Dandekar CR, Shin YC (2013) Experimental evaluation of laser-assisted machining of silicon carbide particle-reinforced aluminum matrix composites. Int J Adv Manuf Technol 66:1603–1610
20. Bejjani R, Shi B, Attia H, Balazinski M (2011) Laser assisted turning of titanium metal matrix composite. CIRP Ann Manuf Technol 60:61–64
21. Przestacki D (2014) Conventional and laser assisted machining of composite A359/20SiCp. Procedia CIRP 14:229–233
22. Przestacki D, Szymanski P, Wojciechowski S (2016) Formation of surface layer in metal matrix composite A359/20SiCP during laser assisted turning. Compos A: Appl Sci Manuf 91:370–379
23. Kong X, Yang L, Zhang H, Chi G, Wang Y (2016) Optimization of surface roughness in laser-assisted machining of metal matrix composites using Taguchi method. Int J Adv Manuf Technol 85(1–14):365–379
24. Rozzi JC, Pfefferkorn FE, Shin YC, Incropera FP (2000) Experimental evaluation of the laser assisted machining of silicon nitride ceramics. J Manuf Sci Eng Trans he ASME 122:666–670
25. Lei S, Shin YC, Incropera FP (2001) Experimental investigation of thermo-mechanical characteristics in laser-assisted machining of silicon nitride ceramics. J Manuf Sci Eng Trans ASME 123:639–646
26. Rebro PA, Shin YC, Incropera FP (2004) Design of operating conditions for crackfree laser-assisted machining of mullite. Int J Mach Tools Manuf 44:677–694
27. Pfefferkorn FE, Shin YC, Tian Y, Incropera FP (2004) Laser-assisted machining of magnesia-partially-stabilized zirconia. J Manuf Sci Eng 126:42–51

28. Chang C, Kuo C (2007) Evaluation of surface roughness in laser-assisted machining of aluminum oxide ceramics with Taguchi method. Int J Mach Tools Manuf 47:141–147
29. Chang C, Kuo C (2007) An investigation of laser-assisted machining of Al2O3 ceramics planing. Int J Mach Tools Manuf 47:452–461
30. Kim J, Lee S, Suh J (2011) Characteristics of laser assisted machining for silicon nitride ceramic according to machining parameters. J Mech Sci Technol 25:995–1001
31. Roostaei H, Movahhedy MR (2016) Analysis of heat transfer in laser assisted machining of slip cast fused silica ceramics. Procedia CIRP 46:571–574
32. Mia M, Dhar NR (2017) Optimization of surface roughness and cutting temperature in high-pressure coolant-assisted hard turning using Taguchi method. Int J Adv Manuf Technol 88:739–753
33. Rashid WB, Goel S, Davim JP, Joshi SN (2016) Parametric design optimization of hard turning of AISI 4340 steel (69 HRC). Int J Adv Manuf Technol 82:451–462
34. Zębala W, Kowalczyk R (2015) Estimating the effect of cutting data on surface roughness and cutting force during WC-Co turning with PCD tool using Taguchi design and ANOVA analysis. Int J Adv Manuf Technol 77:2241–2256
35. Rebro PA, Shin YC, Incropera FP (2002) Laser-assisted machining of reaction sintered mullite ceramics. J Manuf Sci Eng Trans ASME 124:875–885

Publisher's Note